J. Fluid Mech. (1989), *vol.* 200, *pp.* 265–282
Printed in Great Britain

Slot suction from inviscid channel flow

By J. N. DEWYNNE†, S. D. HOWISON†, J. R. OCKENDON†, L. C. MORLAND‡ AND E. J. WATSON‖

† Mathematical Institute, 24–29 St. Giles, Oxford, OX1 3LB, UK

‡ Department of Engineering Science, Parks Road, Oxford, UK

‖ Mathematics Department, Manchester University, M13 9PL, UK

(Received 26 November 1987 and in revised form 22 June 1988)

Motivated by a problem in turbine blade cooling, we consider suction from an inviscid channel flow into a slot in the channel wall. The flow is assumed to separate smoothly from the leading edge of the slot and the pressure in the stagnant separated region controls the suction. The mass flux into the slot is found in terms of the pressure; for small values of this flux the predicted flow pattern is found to be quite different from that which would result if there were no separated region. In particular, the stagnation point never penetrates more than approximately 0.05 slot widths into the slot.

1. Introduction

We consider the flow that is set up when fluid is extracted from a crossflow into a slot. The practical motivation for the study arises from the analysis of the film cooling of gas turbine blades. In this process cool air is sucked from a channel inside the blade, through a slot or hole and emitted at the blade surface, where it forms an insulating layer protecting the blade from the hot gases inside the turbine. This permits higher turbine entry temperatures and leads to increased turbine power and efficiency of operation. An important parameter in this process is the mass flow of cool air out of the slot, as this influences the effectiveness of the insulation. It is also important to understand the behaviour of the fluid flow in the channel and slot in order to carry out boundary-layer heat transfer calculations to determine the thermal behaviour of the turbine blade. In this paper we consider a simple inviscid model for the two-dimensional flow in a channel of infinite length with a slot of infinite depth perpendicular to the channel. Our primary interest is the case of weak suction and we demonstrate that a linearized theory is appropriate under such conditions. The complementary problem of the injection of fluid from a slot into a crossflow has been considered by Fitt, Ockendon & Jones (1985), and Morland (1986), also in the context of film cooling.

With reference to figure 1, we consider the following problem. An ideal incompressible irrotational fluid flows along an infinitely long channel of width H, to which there is attached an infinitely deep slot of width L. Fluid is drawn into the slot where the static pressure is held lower than that in the channel. Under these conditions our preliminary experiments† suggest that the pressure along the upstream wall of the slot is constant; our model is thus one of a free shear layer

† In the *injection* problem, flow visualization was performed by injecting hot gas into the wind tunnel and monitoring its progress with heat-sensitive liquid crystals on the tunnel walls. This technique revealed the flow of the injected fluid and the sharpness of the free shear layer. Similar information would be valuable for the suction problem but it would involve heating the tunnel flow. For this reason a different experimental procedure has been devised, and it is hoped to publish a description, together with experimental results, in a subsequent paper.

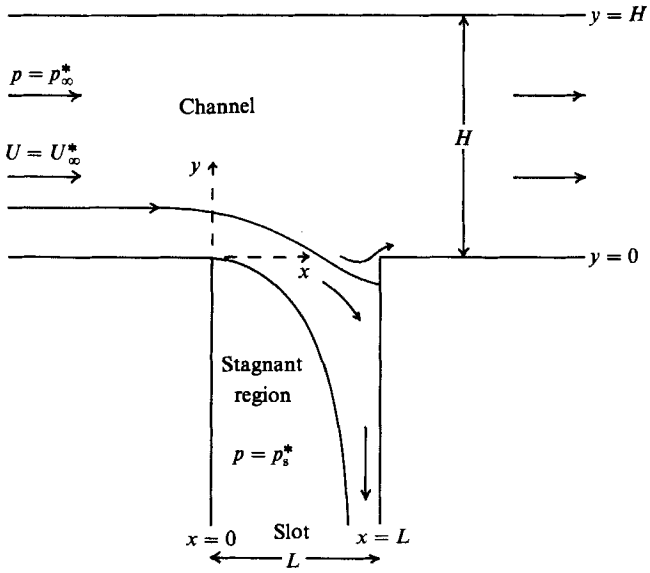

FIGURE 1. Geometry of idealized slot-suction problem.

separating from the leading corner of the slot and dividing a region of stagnant fluid from the flow in the slot. We assume as a Kutta condition that this free shear layer separates smoothly from the leading corner so that the velocity there remains finite. The flow is also assumed to be uniform in the far field in both the channel and the separated region.

If the upstream static pressure is denoted by p^*_∞ and the static pressure in the stagnant zone of the slot by p^*_s, with $p^*_\infty > p^*_s$, the fluid speed along the free shear layer U^*_s is given by Bernoulli's equation as

$$U^{*2}_s = U^{*2}_\infty + (p^*_\infty - p^*_s)/\tfrac{1}{2}\rho,$$

where U^*_∞ is the upstream velocity and ρ the fluid density. We note that in the context of our experiments and film cooling, it is the pressure difference $p^*_\infty - p^*_s$ that can be controlled most conveniently. Non-dimensionalizing distance with respect to L, velocity with respect to the upstream channel speed U^*_∞ and pressure with respect to $\frac{1}{2}\rho U^{*2}_\infty$, we obtain the following free boundary problem for the stream function $\psi(x, y)$ and free shear layer $y = S(x)$;

$$\nabla^2\psi = 0 \quad \text{in} \quad \Omega, \tag{1.1a}$$

$$\psi = 0 \quad \text{on} \quad y = 0, x < 0 \quad \text{and} \quad y = S(x), 0 \leqslant x < x^*, \tag{1.1b}$$

$$\psi = m \quad \text{on} \quad x = 1, y < 0 \quad \text{and} \quad y = 0, x > 1, \tag{1.1c}$$

$$\psi = h \quad \text{on} \quad y = h, -\infty < x < \infty, \tag{1.1d}$$

$$|\nabla\psi| = c \quad \text{on} \quad y = S(x), 0 < x < x^*, \tag{1.1e}$$

$$\psi \to y \quad \text{as} \quad x \to -\infty, 0 \leqslant y \leqslant h, \tag{1.1f}$$

$$\psi \to m + (1 - m/h)\, y \quad \text{as} \quad x \to \infty, 0 \leqslant y \leqslant h, \tag{1.1g}$$

$$S(0) = S'(0) = 0, \quad S(x) \to -\infty \quad \text{as} \quad x \uparrow x^* < 1, \tag{1.1h}$$

where $$\Omega = \{-\infty < x < \infty, 0 < y < h\} \cup \{S(x) < y \leqslant 0; \quad 0 < x < 1\},$$

$h = H/L$ is the non-dimensional channel width, c the non-dimensional speed of the fluid at the shear layer and m denotes the mass flow rate into the slot. The value of x^* is determined by $x^* = 1 - m/c$, by mass conservation. For notational convenience, we take $S(x) = -\infty$ for $x^* < x < 1$. Unless the separating streamline attaches at the trailing corner of the slot, the flow will have infinite velocity at that corner.

In terms of the non-dimensional parameter

$$\epsilon^2 = (p_\infty^* - p_s^*)/\tfrac{1}{2}\rho U_\infty^{*2} \tag{1.2}$$

c^2 may be written as

$$c^2 = 1 + \epsilon^2. \tag{1.3}$$

Since ϵ^2 measures the strength of suction, it is clear that high suction results in high shear-layer speed $c \gg 1$, while small suction gives $c \sim 1$. In view of the ability to control $p_\infty^* - p_s^*$, we regard c as our independent variable and m, the mass flow, as a dependent variable.

The free boundary problem (1.1) is amenable to standard complex variable techniques. In the absence of a crossflow in the channel there is a well-known symmetric solution with free boundaries separating smoothly from each corner (Michell 1890; Milne-Thomson 1968; Birkhoff & Zarantonello 1957). The presence of the crossflow, however, eliminates the possibility of such a symmetric solution. In other related work, Watson (1946) considers the behaviour of jets issuing from a stepped aperture into free space, rather than into a slot, showing that for the plane aperture with crossflow, the jet formed is at an acute angle to the crossflow. This suggests the further consequence that, not only is the flow in the slot asymmetric, but that smooth separation from both the leading and trailing corners is only compatible with two separated regions extending infinitely far into the slot when the slot is at an acute angle calculated by Michell (1890) as a function of c. For slots inclined at other angles, either upstream or downstream, we can either postulate just one separated region (as in this paper) or we must allow the stream flowing into the slot to reattach to the appropriate slot wall at some finite distance.

When separated regions are ignored, the problem reduces to that of flow in a branched canal one aspect of which has been considered in Milne-Thomson (1968).

If the suction strength is small, a linearized analysis of (1.1) is possible. We assume in §2 that the flow in the channel is a parallel flow perturbed by the suction, and seek an expansion in the parameter ϵ^2. The theory is valid except in the neighbourhood of the trailing corner and the stagnation point, and we assume that the stagnation point lies in an $O(\epsilon^2)$ neighbourhood of the trailing corner. In §3 we shall show that the separating streamline can only attach at the trailing corner for a unique pair $c = c^*$ and $m = m^*$ (assuming h fixed) and we shall obtain these values analytically for an open channel ($h = \infty$) and numerically for a closed channel ($h < \infty$). In §4 we consider the behaviour of the stagnation point and mass flow in the case $c < c^*$, with particular emphasis on the limit $c \to 1$ and the open channel. The main result of this analysis is that the stagnation point is shown to have non-monotone dependence on c, moving down the rear slot wall as c falls below c^*, then back up towards the trailing corner as $c \to 1$. The asymptotic behaviours of the mass flow and free shear layer agree with those predicted by the linearized theory, and it is shown that the stagnation point does indeed lie within an $O(\epsilon^2)$ neighbourhood of the trailing corner. The non-monotone behaviour of the stagnation point is due to the shear layer, and should be contrasted with the corresponding problem without separation, where the stagnation point moves monotonically and indefinitely down the rear slot wall as the slot mass

flow tends to zero. In §5 we consider the strong suction case $c > c^*$. Since the details of the calculations are essentially identical to those of §4, only the results are noted.

2. Linearized theory

In the small suction limit, the parameter ϵ^2 given by (1.2) and the mass flow into the slot, m, will be small. Under these circumstances it is apparent that the effect of the slot suction will be an $O(\epsilon^2)$ perturbation to a uniform parallel flow in the channel, except in an $O(\epsilon^2)$ neighbourhood of the trailing corner and stagnation point. In developing the linearized model, it is convenient to work in terms of the velocity potential $\Phi(x, y)$ of the channel flow. We do not attempt to match the channel flow to the slot flow as this involves an analysis of the flow in the neighbourhood of the stagnation point and a considerable loss of simplicity. Since the linearized model will be shown to predict correctly the asymptotic mass flow into the slot, it also correctly implies that the far-field slot flow is a uniform jet of width $O(\epsilon^2)$ moving parallel to the rear slot wall at speed $c \approx 1+\frac{1}{2}\epsilon^2$. Assuming the effects of the slot suction result in $O(\epsilon^2)$ perturbations to the otherwise parallel channel flow we write

$$\Phi(x, y) \sim x+\epsilon^2\varphi(x, y)+O(\epsilon^4), \tag{2.1}$$

where $\varphi(x, y)$ denotes the perturbation potential. Linearizing the Bernoulli equation gives

$$p = p_\infty - 2\epsilon^2\frac{\partial\varphi}{\partial x}+O(\epsilon^4) \tag{2.2}$$

for the non-dimensional pressure p, where p_∞ denotes the non-dimensional upstream channel static pressure.

Along the free shear layer we have no normal flow and constant prescribed velocity $c = 1+\frac{1}{2}\epsilon^2+O(\epsilon^4)$. Together with (2.1) these conditions imply that, in the region of validity of (2.1), the displacement of the shear layer from the plane $y = 0$ is $O(\epsilon^2)$. Writing the shear layer as

$$y = \epsilon^2 S_1(x)+O(\epsilon^4), \quad 0 < x < 1, \tag{2.3}$$

the linearized condition of tangential flow along the shear layer gives

$$S_1'(x) = \frac{\partial\varphi}{\partial y}(x, 0)+O(\epsilon^2), \quad 0 < x < 1, \tag{2.4}$$

while continuity of pressure or, equivalently, prescription of fluid speed on the shear layer linearizes to give

$$\frac{\partial\varphi}{\partial x}(x, 0) = \tfrac{1}{2}, \quad 0 < x < 1. \tag{2.5}$$

The perturbation potential φ must satisfy Laplace's equation in the channel, and it must behave as a sink in the far field. Furthermore, $\partial\varphi/\partial y$ must vanish on all rigid boundaries of the channel, and $(\partial\varphi/\partial y)(x, 0)$ must be continuous and zero at $x = 0$ in order that the shear layer separate smoothly.

For a channel of finite width h,

$$\nabla^2\varphi = 0 \quad \text{in} \quad 0 < y < h, -\infty < x < \infty,$$

$$\frac{\partial\varphi}{\partial y}(x,0) = 0 \quad \text{on} \quad x \leqslant 0, x > 1,$$

$$\frac{\partial\varphi}{\partial y}(x,h) = 0, \quad -\infty < x < \infty,$$

$$\frac{\partial\varphi}{\partial x}(x,0) = \tfrac{1}{2}, \quad 0 < x < 1,$$

and as $x \to -\infty$ we require

$$\lim_{x\to-\infty}\frac{\partial\varphi}{\partial x}(x,y) = 0, \quad 0 \leqslant y \leqslant h;$$

$(\partial\varphi/\partial x)(\infty, y)$ is a finite constant to be determined by mass conservation. Applying the mapping $\zeta = e^{\pi z/h}$ we obtain the least singular solution

$$\frac{\partial\varphi}{\partial x} - i\frac{\partial\varphi}{\partial y} = \frac{1}{2}\left\{1 - e^{\pi/2h}\left[\frac{(e^{\pi z/h}-1)}{(e^{\pi z/h}-e^{\pi/h})}\right]^{\frac{1}{2}}\right\}. \tag{2.6}$$

The pressure along the channel wall, $y = 0$, may be calculated from (2.2) and (2.6) and is

$$p = p_\infty - \epsilon^2 e^{\pi/2h}\left[\frac{e^{\pi x/h}-1}{e^{\pi x/h}-e^{\pi/h}}\right]^{\frac{1}{2}}, \quad x < 0, x > 1; \tag{2.7}$$

the mass flow into the slot is found to be

$$m = -\epsilon^2\int_0^1 \frac{\partial\varphi}{\partial y}(x,0)\,dx = \tfrac{1}{2}h\epsilon^2(e^{\pi/2h}-1). \tag{2.8}$$

In the limit $h \to \infty$ we require that $\varphi = O(\log r)$ as $r = (x^2+y^2)^{\frac{1}{2}} \to \infty$, and we find that

$$m = \tfrac{1}{4}\pi\epsilon^2, \tag{2.9a}$$

$$S_1 = \tfrac{1}{2}[(x(1-x))^{\frac{1}{2}} - \sin^{-1}x^{\frac{1}{2}}]. \tag{2.9b}$$

3. Stagnation point at the trailing corner

In the linearized theory of the previous section, it is assumed that the stagnation point lies within an $O(\epsilon^2)$ neighbourhood of the trailing corner. In this and the following two sections we examine the dependence of the stagnation point and mass flow m on the speed c. For fixed channel width h, it will become apparent that only for a unique value $c = c^*$ will the dividing streamline attach at the trailing corner. The analysis is much easier in this case and will be presented in this section; it will be subsequently generalized to the cases $c < c^*$ and $c > c^*$, corresponding to weaker and stronger suction respectively.

When the stagnation point is at the trailing corner, the situation is described by problem (1.1) with the extra condition that $|\nabla\varphi| = 0$ at $x = 1, y = 0$. It is shown in figure 2(*a*), and in figures 2(*b*), 2(*c*), 2(*d*) we show the potential (w)-plane, hodograph (Q)-plane and the upper half-plane used to connect them (ζ-plane); here

$$Q = \log\frac{dw}{dz} = \log q - i\theta, \quad z = x+iy, \quad w = \varphi+i\psi.$$

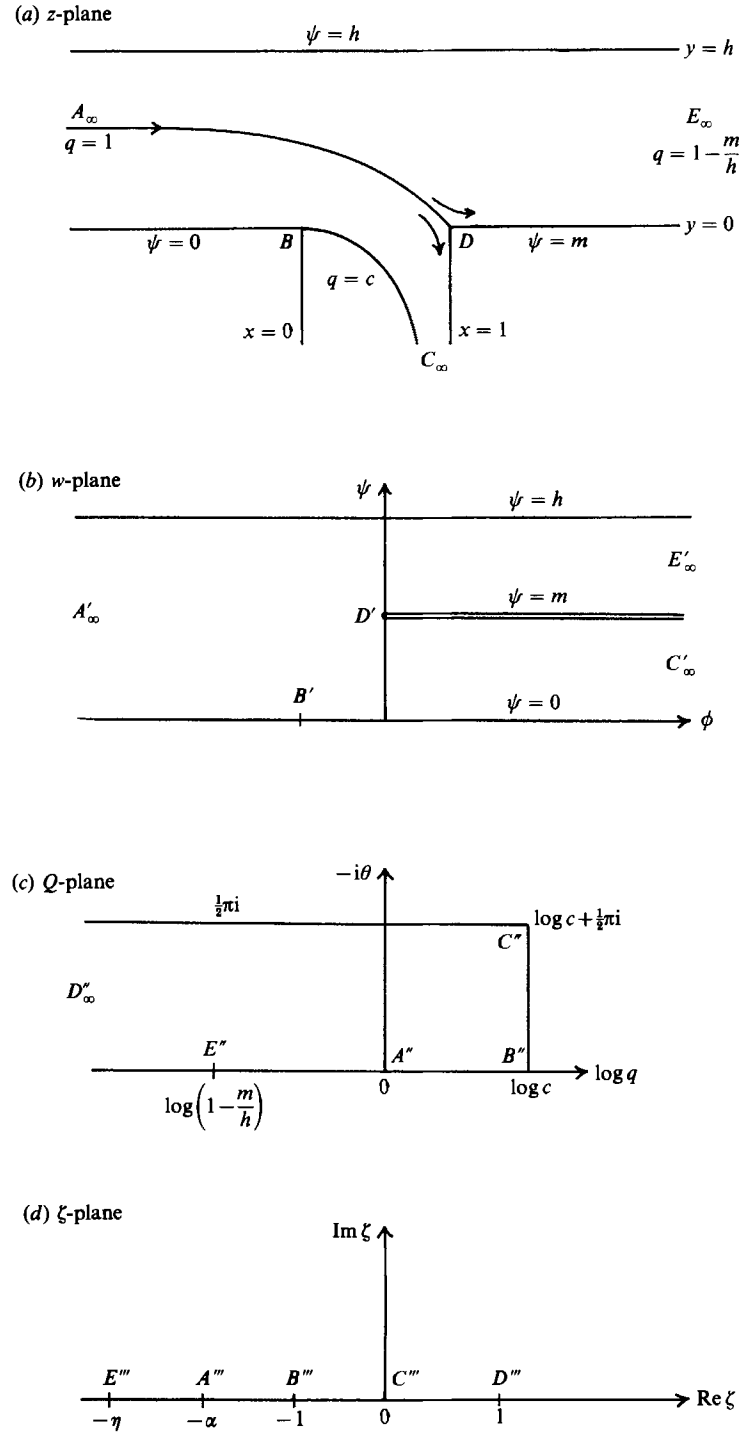

FIGURE 2. Complex planes for the case $c = c^*$.

Applying a Schwarz–Christoffel mapping to transform the upper half of the ζ-plane into the region occupied by the fluid in the w-plane we obtain

$$\frac{\mathrm{d}w}{\mathrm{d}\zeta} = \frac{-m}{\pi}\frac{(1+\alpha)(1+\eta)}{(\zeta+\alpha)(\zeta+\eta)(\zeta-1)}, \tag{3.1}$$

where α, η are as indicated, while mapping the upper half-ζ-plane into the relevant region of the Q-plane we find

$$Q = \tfrac{1}{2}\log(-\zeta+(\zeta^2-1)^{\frac{1}{2}}) + \log c, \tag{3.2}$$

or

$$\zeta = -\cosh 2(Q-\log c). \tag{3.3}$$

The logarithms and square roots are principal valued and $(\zeta^2-1)^{\frac{1}{2}} \sim \zeta$ as $\zeta \to \infty$. The parameters α and η are related to the physical parameters c, h and m by

$$\alpha = \frac{1}{2}\left(c^2+\frac{1}{c^2}\right), \qquad \eta = \frac{1}{2}\left(k^2+\frac{1}{k^2}\right), \tag{3.4a,b}$$

where

$$k = \frac{h-m}{hc} \leqslant \frac{1}{c} < 1. \tag{3.5}$$

To determine α and η (and hence, for fixed h, both c and m) we have the condition that the slot width be unity. Since

$$\begin{aligned}\mathrm{d}z &= \mathrm{e}^{-Q}\frac{\mathrm{d}w}{\mathrm{d}\zeta}\frac{\mathrm{d}\zeta}{\mathrm{d}Q}\mathrm{d}Q \\ &= \frac{-2m}{\pi}(1+\alpha)(1+\eta) \\ &\quad \times \frac{\mathrm{e}^{-Q}\sinh 2(Q-\log c)\,\mathrm{d}Q}{(\alpha-\cosh 2(Q-\log c))(\eta-\cosh 2(Q-\log c))(1+\cosh 2(Q-\log c))},\end{aligned}$$

this condition becomes

$$\begin{aligned}1 &= \frac{-2m}{\pi}(1+\alpha)(1+\eta)\int_{B''}^{D''_\infty} \\ &\quad \times \frac{\mathrm{e}^{-Q}\sinh 2(Q-\log c)\,\mathrm{d}Q}{(\alpha-\cosh 2(Q-\log c))(\eta-\cosh 2(Q-\log c))(1+\cosh 2(Q-\log c))},\end{aligned}$$

where the path of integration lies inside the region of the Q-plane indicated in figure 2(*c*). Noting that $B'' = \log c$, $D''_\infty = -\infty + \frac{1}{2}\pi\mathrm{i}$ and putting $\omega = \mathrm{e}^{(Q-\log c)}$ we find that

$$1 = \frac{8m}{\pi c}(1+\alpha)(1+\eta)\int_0^1 \frac{\omega^2(\omega^2-1)}{(\omega^2+1)(\omega^2-c^2)(\omega^2-1/c^2)(\omega^2-k^2)(\omega^2-1/k^2)}\mathrm{d}\omega, \tag{3.6}$$

where the path of integration lies in the upper half-ω-plane and to the right of $\mathrm{Re}\,\omega = 0$. The integral may be evaluated explicitly and shown to have imaginary component

$$\tfrac{1}{2}\pi k^2c^2\frac{c^3(1+k^2)^2-k(1+c^2)^2}{(1+c^2)^2(1+k^2)^2(k^2-c^2)(k^2c^2-1)} \tag{3.7}$$

and real component

$$\frac{c^2}{2(1+c^2)^2}\frac{k^2}{(1+k^2)^2}\left\{\pi+\frac{(c^2+1)(k^2+1)}{(c^2-k^2)(k^2c^2-1)}\left[k(1+c^2)\log\left(\frac{1+k}{1-k}\right)-c(1+k^2)\log\left(\frac{c+1}{c-1}\right)\right]\right\}. \tag{3.8}$$

h	c^*	m^*
∞	1.7321	0.6282
100	1.7266	0.6262
10	1.6788	0.6084
5	1.6280	0.5885
1	1.3130	0.4412
0.5	1.1109	0.3094
0.2	1.0017	0.1406
0.1	1.0000	0.0704

TABLE 1. Values of c^* and m^* necessary for separating streamline to attach at trailing edge, as functions of channel width h

For a channel of finite width ($k < 1/c$) the condition that (3.7) vanish is

$$\frac{k}{(1+k^2)^2} = \frac{c^3}{(1+c^2)^2}. \tag{3.9}$$

For $c = \sqrt{3}$, (3.9) has the unique solution $k = 1/\sqrt{3}$; otherwise (3.9) has two solutions, $k = 1/c$ and $k = 1/c_1$ where $c_1 \neq c$ satisfies $c_1^3/(1+c_1^2)^2 = c^3/(1+c^2)^2$. Since for $c \geqslant 0$, $c^3/(1+c^2)^2$ increases monotonically from zero until $c = \sqrt{3}$, then decreases monotonically to zero as $c \to \infty$, c_1 exists and is unique. It follows that it is possible to solve (3.9) subject to the physically necessary condition $k \leqslant 1/c$ only if $c \leqslant \sqrt{3}$. If $c \leqslant \sqrt{3}$, there exists a unique k satisfying (3.9) and $k \leqslant 1/c$. Thus (3.6) becomes

$$1 = \frac{m}{\pi c}\left\{\pi + \frac{(c^2+1)(k^2+1)}{(c^2-k^2)(c^2k^2-1)}\left[(1+c^2)\,k\log\left(\frac{1+k}{1-k}\right) - c(1+k^2)\log\left(\frac{c+1}{c-1}\right)\right]\right\}, \tag{3.10}$$

uniquely determining m. With $1 < c \leqslant \sqrt{3}$ given, and with k and m determined by (3.9) and (3.10), h follows from (3.5). Conversely, fixing h, then c, k, m are uniquely determined by (3.5), (3.9) and (3.10), implying that with h fixed there are unique vaues of c and m such that the stagnation point lies on the trailing corner. In table 1 we list these values as functions of h, obtained by solving (3.5), (3.9) and (3.10) numerically.

Results for the open channel follow by letting h approach infinity. In this limit $\eta \to \alpha$ and $k \to 1/c$, reducing (3.6) to

$$\begin{aligned} 1 &= \frac{8m}{\pi c}(1+\alpha)^2 \int_0^1 \frac{\omega^2(\omega^2-1)\,\mathrm{d}\omega}{(\omega^2+1)(\omega^2-c^2)^2(\omega^2-1/c^2)^2} \\ &= \frac{m}{\pi c}\left\{\pi + \left(\frac{c^2+1}{c^2-1}\right)^2 + \frac{1+c^2}{2c}\log\left(\frac{c+1}{c-1}\right) + \tfrac{1}{2}\pi\mathrm{i}c\left(\frac{c^2-3}{c^2-1}\right)\right\}, \end{aligned} \tag{3.11}$$

where again the path of integration has been taken in the upper-right quadrant of the ω-plane. In order that the imaginary component vanish in (3.11) we require

$$c^2 = 3 = c^{*2} \tag{3.12}$$

and

$$m = \pi\sqrt{3}\Big/\left(4+\pi+\frac{2}{\sqrt{3}}\log\frac{\sqrt{3}+1}{\sqrt{3}-1}\right) = m^*, \tag{3.13}$$

say. These results also follow from (3.5), (3.7) and (3.8) by letting $h \to \infty$ and $\alpha \to \eta$.

If we now assume that $c \sim 1+\frac{1}{2}\epsilon^2$ for small $\epsilon > 0$, then as M. B. Glauert (1987, private communication) has observed, we find that to leading order (3.11) reduces to

$$m \approx \tfrac{1}{4}\pi\epsilon^4 + O(\epsilon^6)$$

but the neglected higher-order terms have non-zero imaginary parts. The interpretation of this is that the leading and trailing edges must no longer be level, differing by a height of $O(\epsilon^2)$. The observation does, however, suggest that at small suction strength the stagnation point lies in a small neighbourhood of the trailing corner. As we demonstrate in the following section, this result is qualitatively correct, but predicts an incorrect asymptotic relationship between c and m (see (4.15)), namely that $m = O((c^2-1)^2)$.

4. The case $c < c^*$

As the upstream channel static pressure and the static pressure in the stagnant region of the slot are independent, it is possible to vary the fluid speed on the free shear layer, c. In particular, it is possible for c to assume values other than c^*, in which case the stagnation point will not lie on the trailing slot corner. For very strong suction (i.e. $m \to h$), most of the fluid is drawn into the slot and we expect the stagnation point to lie far along the downstream channel wall, with fluid being drawn back into the slot. In the limit $m = h$ the stagnation point must be at $x = \infty$. If this were not so, the dividing streamline would separate a stagnant downstream channel region, where ψ would be constant, from a mobile upstream region, where ψ would vary. Such a situation is inconsistent with ψ being harmonic in the whole channel. For weak suction ($m \to 0, c \to 1$) the behaviour of the stagnation point is less obvious. In both cases, however, the fluid speed at the trailing slot corner will be infinite according to this model.

In order to analyse either case, a hodograph plane more general than that used in §3 is necessary. Specifically, in order to align the trailing and leading slot corners an additional parameter in the mapping is necessary. This parameter can only be introduced if there is a local minimum in fluid speed distinct, in general, from the stagnation point. Such a point of minimum speed must occur on the slot or channel walls and the only consistent configuration is for it to lie along the downstream channel wall when the stagnation point is on the rear slot wall and vice versa.

In figure 3 we show the physical (z), potential (w) and hodograph (Q) planes corresponding to the case in which the stagnation point, S, lies along the rear slot wall. This corresponds to the relatively weak suction case $c < c^*$ and will be treated in more detail than the strong suction case $c > c^*$, the results for the latter case being summarized in the following section.

When $c < c^*$ the point of local speed minimum is located along the downstream channel wall, and is denoted by T in figure 3. The z-, w- and Q-planes are connected by the ζ-plane shown in figure 3(d). We find that

$$\frac{\mathrm{d}w}{\mathrm{d}\zeta} = \frac{\alpha m \eta}{\pi s} \frac{\zeta - s}{\zeta(\zeta-\alpha)(\zeta-\eta)},$$

$$Q = \log\left(\frac{(\zeta(s+1))^{\frac{1}{2}} - (s(\zeta+1))^{\frac{1}{2}}}{(\zeta(s+1))^{\frac{1}{2}} + (s(\zeta+1))^{\frac{1}{2}}}\right) - \log\left(\frac{(\zeta-1)^{\frac{1}{2}}}{(2\zeta)^{\frac{1}{2}} + (\zeta+1)^{\frac{1}{2}}}\right) + \log c,$$

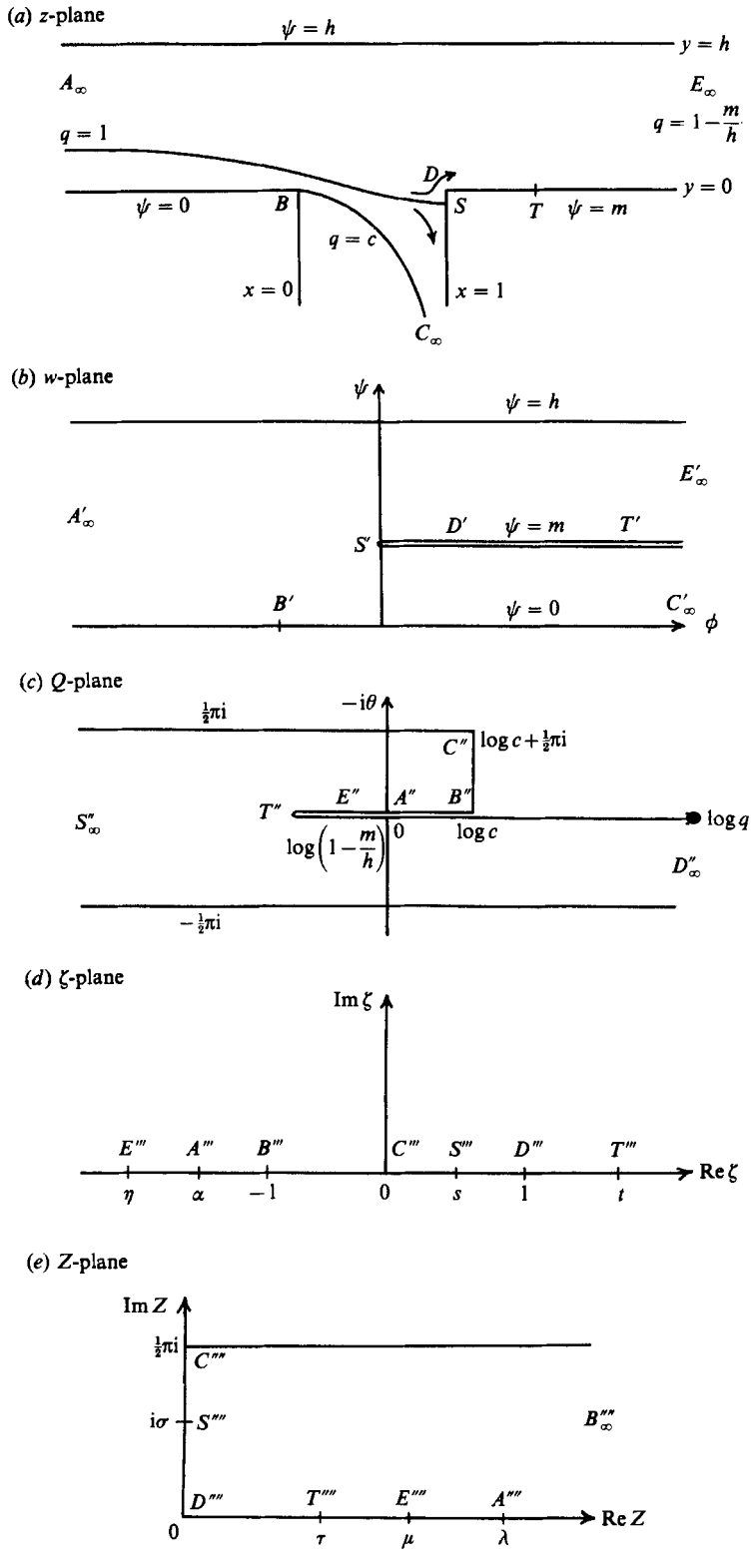

FIGURE 3. Complex planes for the case $c < c^*$.

where the mapping parameters α, η are related to the physical parameters c, h, m and to t by

$$c = \frac{(\alpha-1)^{\frac{1}{2}}}{(2\alpha)^{\frac{1}{2}}+(\alpha+1)^{\frac{1}{2}}} \frac{[(\alpha(s+1))^{\frac{1}{2}}+(s(\alpha+1))^{\frac{1}{2}}]^2}{\alpha-s}, \tag{4.1a}$$

$$k = \frac{\eta-s}{[(\eta(s+1))^{\frac{1}{2}}+(s(\eta+1))^{\frac{1}{2}}]^2} \frac{(2\eta)^{\frac{1}{2}}+(\eta+1)^{\frac{1}{2}}}{(\eta-1)^{\frac{1}{2}}}, \tag{4.1b}$$

$$t = \frac{(2s(s+1))^{\frac{1}{2}}-s}{(2s(s+1))^{\frac{1}{2}}-1}, \tag{4.1c}$$

with k given by (3.5). The slot width condition is

$$1 = \frac{\alpha\eta m}{\pi s c} \int_{-1}^{1} \frac{[(s(\zeta+1))^{\frac{1}{2}}+(\zeta(s+1))^{\frac{1}{2}}]^2}{\zeta(\zeta-\alpha)(\zeta-\eta)} \frac{(\zeta-1)^{\frac{1}{2}}}{(2\zeta)^{\frac{1}{2}}+(\zeta+1)^{\frac{1}{2}}} \mathrm{d}\zeta \tag{4.2}$$

where the path of integration lies in the upper half of the ζ-plane. The position of the stagnation point, z_s, is then determined from

$$z_s = 1 - \frac{\alpha\eta m}{\pi s c} \int_{s}^{1} \frac{[(s(\zeta+1))^{\frac{1}{2}}+(\zeta(s+1))^{\frac{1}{2}}]^2}{\zeta(\zeta-\alpha)(\zeta-\eta)} \frac{(\zeta-1)^{\frac{1}{2}}}{(2\zeta)^{\frac{1}{2}}+(\zeta+1)^{\frac{1}{2}}} \mathrm{d}\zeta, \tag{4.3}$$

with the path of integration along the real axis. The parameters α, η and s and m are determined as functions of c and h by (4.1*a*, *b*), (4.2) and (3.5). It is interesting to note that since $|t| > 1$, as is clear from figure 3, it follows that $\frac{1}{7} < s < 1$, so that the image of the stagnation point is bounded away from the image of the slot base C, in the ζ-plane.

To proceed further analytically, we put

$$\zeta = \frac{\cosh^2 Z}{2-\cosh^2 Z},$$

which maps the upper half-ζ-plane into the semi-infinite rectangle shown in figure 3(*e*), and put

$$\alpha = \frac{\cosh^2\lambda}{2-\cosh^2\lambda}, \quad \eta = \frac{\cosh^2\mu}{2-\cosh^2\mu}, \quad t = \frac{\cosh^2\tau}{2-\cosh^2\tau}, \quad s = \frac{\cos^2\sigma}{2-\cos^2\sigma}. \tag{4.4}$$

Equations (4.1) then become

$$c = \frac{\sinh\lambda}{\cosh\lambda+1} \frac{\cosh\lambda+\cos\sigma}{\cosh\lambda-\cos\sigma}, \tag{4.5a}$$

$$k = \frac{\sinh\mu}{\cosh\mu-1} \frac{\cosh\mu-\cos\sigma}{\cosh\mu+\cos\sigma}, \tag{4.5b}$$

$$\cosh^2\tau = \frac{\cos\sigma(2-\cos\sigma)}{2\cos\sigma-1}. \tag{4.5c}$$

Inspection of figure 3 shows that $0 \leqslant \tau \leqslant \mu$, $\mu < \lambda$ (unless $h = \infty$, in which case $\mu = \lambda$) and $0 \leqslant \sigma \leqslant \frac{1}{2}\pi$. A consequence of $\tau \geqslant 0$ and (4.5*c*) is that $0 \leqslant \sigma < \frac{1}{3}\pi$, a result equivalent to $\frac{1}{7} < s \leqslant 1$.

The slot width integral (4.2) becomes

$$1 = \frac{2m}{\pi c} \frac{\cosh^2\lambda \cosh^2\mu}{\cos^2\sigma} \int_{\infty}^{0} \frac{(\cosh Z-1)(\cosh Z+\cos\sigma)^2 \mathrm{d}Z}{\cosh Z(\cosh^2 Z-\cosh^2\lambda)(\cosh^2 Z-\cosh^2\mu)} \tag{4.6}$$

with the path of integration lying inside the rectangle in figure 3(*e*). The location of the stagnant point is then determined by

$$z_s = 1+\frac{2mi}{\pi c}\frac{\cosh^2\lambda\cosh^2\mu}{\cos^2\sigma}\int_0^{\sigma}\frac{(\cos y-1)(\cos y+\cos\sigma)^2\,\mathrm{d}y}{\cos y(\cosh^2\lambda-\cos^2 y)(\cosh^2\mu-\cos^2 y)}, \tag{4.7}$$

where y is real.

Both integrals (4.6) and (4.7) may be evaluated in terms of elementary functions. The real and imaginary components of (4.6) give, respectively, the equations

$$1 = \frac{m}{\pi c}\left\{\pi+\frac{2\cosh^2\lambda\cosh^2\mu}{\cosh^2\sigma}\frac{f(\lambda,\sigma)-f(\mu,\sigma)}{\cosh^2\lambda-\cosh^2\mu}\right\}, \tag{4.8a}$$

$$0 = \frac{g(\lambda,\sigma)-g(\mu,\sigma)}{\cosh^2\lambda-\cosh^2\mu}, \tag{4.8b}$$

where

$$f(\lambda,\sigma) = \frac{2\lambda}{\sinh 2\lambda}[\sinh^2\lambda+(1-\cos\sigma)^2], \tag{4.9a}$$

$$g(\lambda,\sigma) = \frac{\cosh\lambda-1}{\sinh\lambda}\left(1+\frac{\cos\sigma}{\cosh\lambda}\right)^2. \tag{4.9b}$$

From (4.7) we find that

$$z_s = 1-\frac{2mi}{\pi c}\left[\sinh^{-1}(\tan\sigma)+\frac{\cosh^2\lambda\cosh^2\mu}{\cos^2\sigma}\frac{F(\lambda,\sigma)-F(\mu,\sigma)}{\cosh^2\lambda-\cosh^2\mu}\right], \tag{4.10}$$

where

$$F(\lambda,\sigma) = \left(1+\frac{\cos\sigma}{\cosh\lambda}\right)^2\tanh\frac{\lambda}{2}\tan^{-1}\left(\coth\frac{\lambda}{2}\tan\frac{\sigma}{2}\right) + \left(1-\frac{\cos\sigma}{\cosh\lambda}\right)^2\coth\frac{\lambda}{2}\tan^{-1}\left(\tanh\frac{\lambda}{2}\tan\frac{\sigma}{2}\right). \tag{4.11}$$

By graphical considerations similar to those of §3, it can be established that once λ and σ are specified there is a unique μ satisfying (4.8*b*) and such that $0 \leqslant \mu < \lambda$, provided that $\cos\sigma \geqslant \frac{1}{2}$ and $\cosh\lambda > (\cos\sigma+(17\cos^2\sigma-8\cos\sigma)^{\frac{1}{2}})/2(2\cos\sigma-1)$. Once λ, μ and σ are determined and satisfy (4.8*b*), c, h, m and z_s may be found from (4.5*a*, *b*), (3.5), (4.8*a*) and (4.10).

In table 2 we list values of c, m, z_s, λ, μ, σ obtained numerically for two fixed values of the channel width; $h = 1$ and $h = 10$. The table shows that as c and m decrease from c^* and m^*, the stagnation point initially moves away from the trailing corner and down the rear slot wall. As c and m decrease further, however, the stagnation point turns round and moves back up the slot wall. In the limit $c \to 1, m \to 0$, table 2 suggests that the stagnation point returns to the trailing slot corner. This behaviour should be contrasted with the behaviour of the stagnation point in the absence of the shear layer; in that case the stagnation point moves monotonically down the rear slot wall as $m \to 0$.

To illustrate this point analytically, and to justify the linearized theory of §2, we consider, for simplicity, an open channel. In this case $h = \infty$ and $\mu = \lambda$, making (4.5*a*) and (4.5*b*) equivalent. The transcendental equations for the slot width and stagnation-point position can be obtained by either putting $\mu = \lambda$ in (4.6) and (4.7)

c	m	$(z_s-1)/\mathrm{i}$	λ	μ	σ
		$h=1$			
1.3130	0.4412	0	2.0	0.9089	0
1.0803	0.1527	−0.0448	2.5	1.2041	0.7409
1.0241	0.0578	−0.0445	3.0	1.5691	0.9013
1.0025	0.0078	−0.0114	4.0	2.4581	1.0076
1.0008	0.0028	−0.0046	4.5	2.9433	1.0253
1.0003	0.0010	−0.0018	5.0	3.4366	1.0347
		$h=10$			
1.6788	0.6084	0	1.3728	1.2639	0
1.3947	0.3794	−0.0196	1.4916	1.3753	0.5000
1.1685	0.1825	−0.0532	1.7301	1.6016	0.7500
1.0575	0.0717	−0.0536	2.1039	1.9626	0.9000
1.0087	0.0128	−0.0177	2.8872	2.7343	1.0000
1.0003	0.0004	−0.0008	4.5264	4.3696	1.0400

TABLE 2. Values of m and $(z_s-1)/\mathrm{i}$ for $c \leqslant c^*$ for two finite channel widths $h = 1, 10$

c	m	$(z_s-1)/\mathrm{i}$	λ	σ
1.7321	0.6282	0	1.3170	0
1.5000	0.4489	−0.0158	1.3935	0.4198
1.2500	0.2458	−0.0416	1.5666	0.6739
1.1547	0.1622	−0.0460	1.7100	0.7783
1.1000	0.1109	−0.0431	1.8548	0.8457
1.0100	0.0137	−0.0105	2.7772	0.9981
1.0010	0.0015	−0.0013	3.8435	1.0334
1.0001	0.0002	−0.0001	4.9657	1.0430

TABLE 3. Values of m and $(z_s-1)/\mathrm{i}$ for $c \leqslant c^*$ for an infinite channel

or by taking the limit $\mu \to \lambda$ in (4.8) and (4.10). In either case, the expression (4.5*a*) for c and the conditions for a level unit slot become, after simplification,

$$c = \frac{(\cosh\lambda - 1)\sinh\lambda}{\sinh^2\lambda - \cosh\lambda}, \tag{4.12a}$$

$$1 = \frac{m}{\pi c}\left\{\pi + 4\cosh^2\lambda - 4\cosh\lambda - 6 + \frac{2}{\cosh\lambda - 1} + \frac{2\lambda}{c}\right\}, \tag{4.12b}$$

$$\cos\sigma = \frac{\cosh^2\lambda}{2\sinh^2\lambda - \cosh\lambda}. \tag{4.12c}$$

The position of the stagnation point is then given by

$$z_s = 1 - \frac{2mi}{\pi c}\left\{\sinh^{-1}(\tan\sigma) + \frac{1}{c}\cos^{-1}(\tfrac{1}{2} + \operatorname{sech}\lambda) + \frac{1}{2}\left(\frac{\cosh\lambda - 1}{c^2} - c\sinh\lambda\right)\tan\sigma\right\}, \tag{4.13}$$

while τ is given by (4.5*c*). In table 3 we present values of c, m and z_s, and λ and σ, calculated from (4.12) and (4.13) and plot m and $(z_s-1)/\mathrm{i}$ against $c-1$ in figure 4.

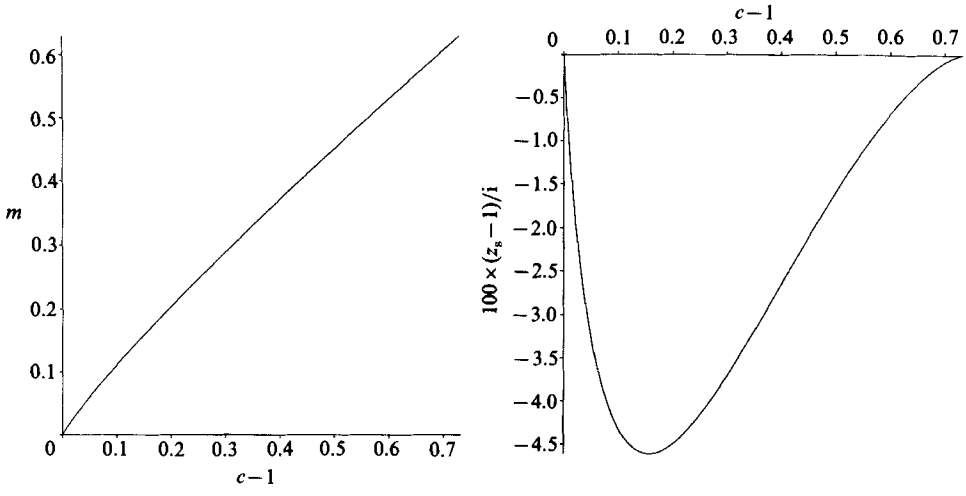

FIGURE 4. Mass flow, m, and stagnation point $(z_s-1)/\mathrm{i}$ as functions of $c-1$ for the open channel with $c \leqslant c^*$.

Inspection of (4.12b) shows that the limit $m \to 0$ can be achieved if either $\cosh\lambda \to \infty$ or $\cosh\lambda \to 1$. The latter case can be excluded as (4.5a) then implies $c < 1$ as $\lambda \to 0$. Thus, we put

$$\cosh\lambda = 1/\epsilon \tag{4.14}$$

and let $\epsilon \to 0$. From (4.12c) we find

$$\cos\sigma \sim \tfrac{1}{2}+\tfrac{1}{4}\epsilon$$

and from (4.12a, b) and (4.13)

$$c \sim 1+\tfrac{1}{2}\epsilon^2, \qquad m \sim \tfrac{1}{4}\pi\epsilon^2, \tag{4.15a, b}$$

$$z_s \sim 1-\tfrac{1}{2}\epsilon^2\mathrm{i}[\log(2+\sqrt{3})+\tfrac{1}{3}\pi-\tfrac{1}{2}\sqrt{3}]. \tag{4.15c}$$

Equation (4.15b) agrees with (2.9a), and the fact that the stagnation point is within an $O(\epsilon^2)$ neighbourhood of the trailing corner is consistent with the linearized theory of §2.

We note that, for the open channel, the free shear layer may be written parametrically as

$$z(r) = \frac{2m\mathrm{i}\cosh^4\lambda}{\pi c\cos^2\sigma}\int_r^\infty \frac{(\mathrm{i}\sinh X-1)(\cos\sigma+\mathrm{i}\sinh X)^2\,\mathrm{d}X}{\sinh X(\sinh^2 X+\cosh^2\lambda)^2}, \tag{4.16}$$

where X is real and r varies from ∞ to zero as $z(r)$ moves from the leading slot edge down to the slot bottom. Applying the slot width condition (4.6) and changing variables to Θ and θ, where $\cosh X = \sinh\lambda\cot\Theta$ and $\cosh r = \sinh\lambda\cot\theta$ (so $0 \leqslant \theta \leqslant \tan^{-1}(\sinh\lambda)$), (4.16) yields

$$x(\theta) = \frac{2m}{\pi c}\left\{\frac{1}{c}(\lambda-\cosh^{-1}(\cosh\lambda\cos\theta)) + \left(1+\frac{1}{c^2}\right)(\cosh\lambda-1)\sinh\lambda(\tanh\lambda-\cos\theta(\cos^2\theta-\operatorname{sech}^2\lambda)^{\frac{1}{2}})\right\}, \tag{4.17a}$$

$$y(\theta) = \frac{-2m}{\pi c}\left\{\tfrac{1}{2}\log\left(\frac{\sinh\lambda+\tan\theta}{\sinh\lambda-\tan\theta}\right)+\frac{\theta}{c}-\frac{\cosh^2\lambda-2}{(\cosh\lambda-1)\sinh\lambda}\sin\theta\cos\theta\right\}, \tag{4.17b}$$

where $z(\theta) = x(\theta) + iy(\theta)$. As $\theta \to 0$, near the leading corner, we find

$$x \sim \frac{m}{\pi c}(2\sinh\lambda - \coth\lambda)^2\theta^2,$$

$$y \sim \frac{-2m}{3\pi c}(2\sinh\lambda - \coth\lambda)\frac{\cosh\lambda + 2}{\sinh^2\lambda}\theta^3,$$

while as $\theta \to \tan^{-1}(\sinh\lambda)$, at the bottom of the slot, we have

$$x \to 1 - \frac{m}{c}, \quad y \to -\infty$$

as we would expect. In the small-mass-flow limit, as $\epsilon \to 0$, we find

$$x = \sin^2\theta + O(\epsilon), \qquad y = \tfrac{1}{2}\epsilon^2(\sin\theta\cos\theta - \theta) + O(\epsilon^3), \tag{4.18}$$

although the limit is only uniform for θ bounded away from $\tan^{-1}(\sinh\lambda)$. Clearly (4.18) and (2.9*b*) are equivalent.

5. The case $c > c^*$

Finally we briefly consider the strong-suction case, where the stagnation point lies along the downstream channel wall. The physical, potential, hodograph, ζ- and Z-planes are shown in figure 5. The position of the local speed minimum is denoted by T. The relations connecting the physical, potential, hodograph and ζ-planes are identical to those given in §4, and (4.1)–(4.3) remain valid. The only distinction between the two cases is that for weak suction $0 < s < 1$ and $|t| > 1$ while for strong suction $0 < t < 1$ and $|s| > 1$ (see figure 5). In terms of Z, related to ζ by $\zeta = \cosh^2 Z/(2 - \cosh^2 Z)$, we find that

$$c = \frac{\sinh\lambda}{\cosh\lambda + 1}\frac{\cosh\lambda + \cosh\sigma}{\cosh\lambda - \cosh\sigma}, \tag{5.1a}$$

$$k = \frac{\sinh\mu}{\cosh\mu - 1}\frac{\cosh\mu - \cosh\sigma}{\cosh\mu + \cosh\sigma}, \tag{5.1b}$$

and

$$\cos^2\tau = \frac{\cosh\sigma(2 - \cosh\sigma)}{2\cosh\sigma - 1}. \tag{5.2}$$

The conditions for a unit width, level slot become

$$1 = \frac{m}{\pi c}\left\{\pi + \frac{2\cosh^2\lambda\cosh^2\mu}{\cosh^2\sigma}\frac{\bar{f}(\lambda,\sigma) - \bar{f}(\mu,\sigma)}{\cosh^2\lambda - \cosh^2\mu}\right\}, \tag{5.3a}$$

$$0 = \frac{\bar{g}(\lambda,\sigma) - \bar{g}(\mu,\sigma)}{\cosh^2\lambda - \cosh^2\mu} \tag{5.3b}$$

where

$$\bar{f}(\lambda,\sigma) = \frac{2\lambda}{\sinh 2\lambda}[\sinh^2\lambda + (\cosh\sigma - 1)^2], \tag{5.4a}$$

$$\bar{g}(\lambda,\sigma) = \frac{\cosh\lambda - 1}{\sinh\lambda}\left(1 + \frac{\cosh\sigma}{\cosh\lambda}\right)^2. \tag{5.4b}$$

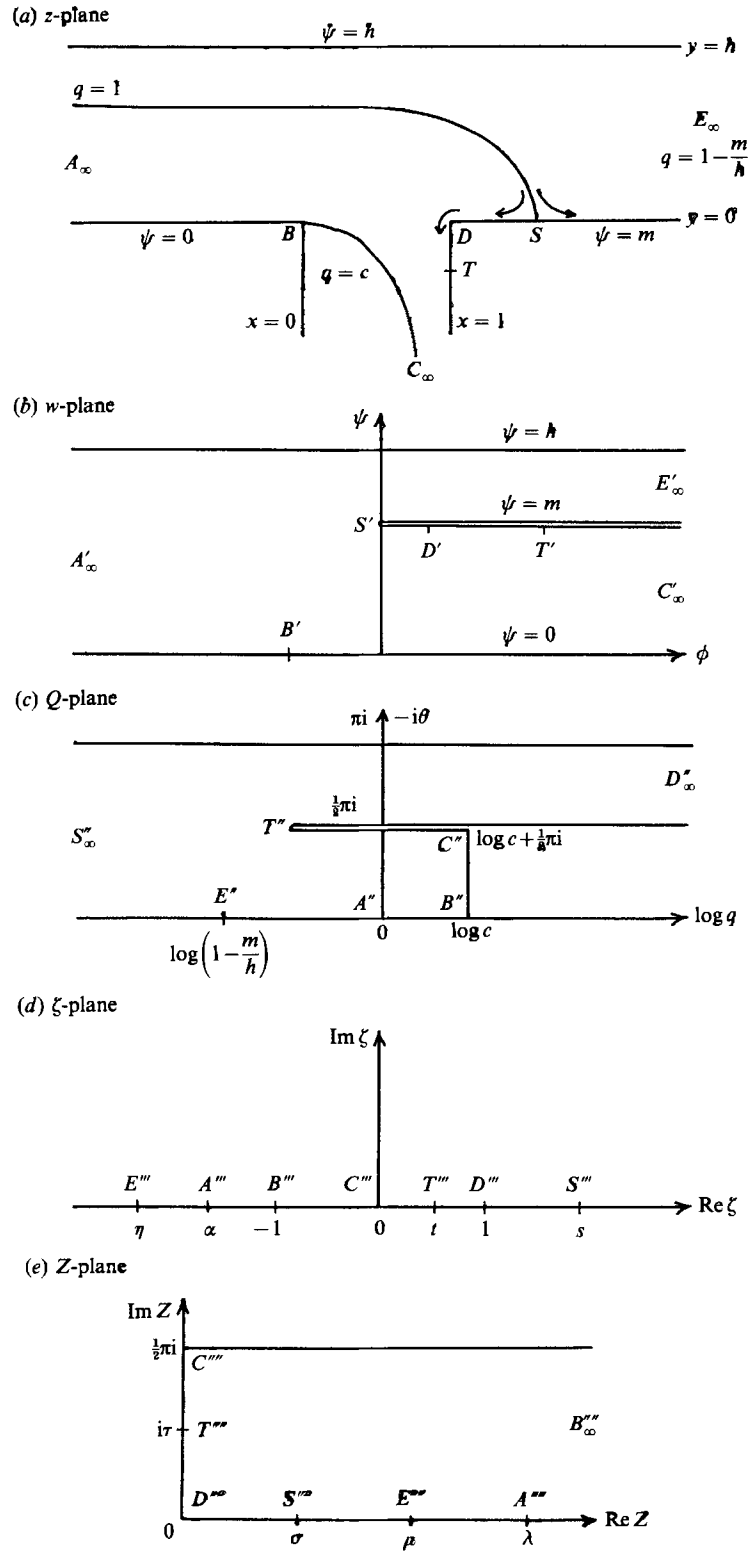

FIGURE 5. Complex planes for the case $c > c^*$.

c	m	z_s	λ	μ	σ
		$h = 1$			
1.3130	0.4412	1	2	0.9089	0
1.5875	0.7303	1.4304	1.8155	0.8170	0.6000
1.7231	0.8668	1.8615	1.7640	0.7921	0.7000
1.8506	0.9925	3.6318	1.7265	0.7750	0.7700
1.8541	0.9962	4.1162	1.7259	0.7743	0.7720
1.8562	0.9982	4.6118	1.7254	0.7741	0.7730
		$h = 10$			
1.6788	0.6084	1	1.3728	1.2639	0
2.4104	1.1706	1.3733	1.2554	1.1549	0.6000
3.6502	2.0995	2.0522	1.1897	1.0942	0.8000
10.366	7.0702	8.3508	1.1252	1.0350	1.0000
12.998	9.0140	15.281	1.1190	1.0293	1.0200
13.888	9.6709	22.265	1.1175	1.0279	1.0250

TABLE 4. Values of m and z_s for $c \geqslant c^*$ for two channels of finite widths $h = 1, 10$

The position of the stagnation point is then determined by

$$z_s = 1 - \frac{2m}{\pi c}\left\{\sin^{-1}(\tanh\sigma) + \frac{\cosh^2\lambda\cosh^2\mu}{\cosh^2\sigma}\frac{\bar{F}(\lambda,\sigma)-\bar{F}(\mu,\sigma)}{\cosh^2\lambda-\cosh^2\mu}\right\}, \tag{5.5}$$

where

$$\bar{F}(\lambda,\sigma) = \left(1+\frac{\cosh\sigma}{\cosh\lambda}\right)^2 \tanh\frac{\lambda}{2}\tanh^{-1}\left(\coth\frac{\lambda}{2}\tanh\frac{\sigma}{2}\right) + \left(1-\frac{\cosh\sigma}{\cosh\lambda}\right)^2 \coth\frac{\lambda}{2}\tanh^{-1}\left(\tanh\frac{\lambda}{2}\tanh\frac{\sigma}{2}\right). \tag{5.6}$$

In table 4 we present numerical values of c, m and z_s obtained from (5.1)–(5.6), for two fixed values of h. Results for an open channel are obtained by letting $\mu \to \lambda$. In this limit we find that the slot width condition (5.3b) becomes

$$\cosh\sigma = \frac{\cosh^2\lambda}{2\sinh^2\lambda - \cosh\lambda} \tag{5.7}$$

while (4.12a, b) remain valid and the position of the stagnation point is

$$z_s = 1 - \frac{2m}{\pi c}\left(\sin^{-1}(\tanh\sigma) + \frac{1}{c}\cosh^{-1}(\tfrac{1}{2}+\operatorname{sech}\lambda) - \frac{1}{2}\left(c\sinh\lambda - \frac{\cosh\lambda - 1}{c^2}\right)\tanh\sigma\right). \tag{5.8}$$

Since σ must lie between 0 and λ, it follows from (5.7) that

$$\tfrac{1}{2}(\sqrt{5}+1) < \cosh\lambda < 2.$$

The limit $\cosh\lambda \to 2$ corresponds to the stagnation point on the trailing corner, while the limit $\cosh\lambda \to \frac{1}{2}(\sqrt{5}+1)$ corresponds to the stagnation point at $x = \infty$ and $c \to \infty$. Thus as $c \to \infty$ we find that

$$m \sim \frac{\pi c}{\pi + \sqrt{5} - 1} + O(1),$$

$$z_s \sim \frac{m}{\pi} + 1 + O(1/c).$$

6. Conclusion

We have presented results for the mass flow into the slot for the entire range of relevant stagnation region pressures c^2-1. For our model, which assumes smooth separation at the leading slot edge, the velocity at the slot trailing edge is unbounded, except at one special value $c = c^*$. When $c > c^*$ the stagnation point is on the channel wall, downstream of the slot, and moves monotonically to infinity with increasing c. If $c < c^*$ the stagnation point is located on the slot downstream wall and it might be expected that, as in the case of the flow without a separation, the stagnation point moves to infinity as the mass flow rate tends to zero. This is found not to be so; the influence of the separation is to prevent the stagnation point from moving further than about 0.05 slot widths into the slot. Preliminary experimental work supports these predictions and we hope to publish the results of this experimental investigation in a subsequent paper.

The authors would like to thank Professor M. B. Glauert for helpful discussions and correspondence. Two of the authors (J.N.D., L.C.M.) acknowledge the support of the Science and Engineering Research Council and one (S.D.H.) support from Shell.

REFERENCES

BIRKHOFF, G. & ZARANTONELLO, E. H. 1957 *Jets, Wakes and Cavities.* Academic.

FITT, A. D., OCKENDON, J. R. & JONES, T. V. 1985 *J. Fluid Mech.* **160**, 15.

MICHELL, J. H. 1890 *Phil. Trans. R. Soc. Lond.* A **181**, 389.

MILNE-THOMSON, L. M. 1968 *Theoretical Hydrodynamics*, 5th edn. Macmillan.

MORLAND, L. C. 1986 Film cooling of turbine blades. M.Sc. Thesis, Oxford University.

WATSON, E. J. 1946 Free Streamline Suction Slots. *Aero. Res. Counc. Tech. Rep.* 2177.